Title

Graph-theoretical analysis of resting-state fMRI in pediatric obsessive–compulsive disorder

Authors

Armstrong, Casey C
Moody, Teena D
Feusner, Jamie D
et al.

Publication Date

2016-03-01

DOI

10.1016/j.jad.2015.12.071

Peer reviewed

HHS Public Access

Author manuscript

J Affect Disord. Author manuscript; available in PMC 2018 January 14.

Published in final edited form as:

J Affect Disord. 2016 March 15; 193: 175–184. doi:10.1016/j.jad.2015.12.071.

Graph-theoretical analysis of resting-state fMRI in pediatric obsessive-compulsive disorder

Casey C. Armstrong[a], **Teena D. Moody**[b], **Jamie D. Feusner**[b], **James T. McCracken**[a], **Susanna Chang**[a], **Jennifer G. Levitt**[a], **John C. Piacentini**[a], and **Joseph O'Neill**[a,*]

[a]Division of Child & Adolescent Psychiatry, UCLA Semel Institute For Neurosciences, Los Angeles, CA, United States

[b]Division of Adult Psychiatry, UCLA Semel Institute For Neurosciences, Los Angeles, CA, United States

Abstract

Background—fMRI graph theory reveals resting-state brain networks, but has never been used in pediatric OCD.

Methods—Whole-brain resting-state fMRI was acquired at 3 T from 21 children with OCD and 20 age-matched healthy controls. BOLD connectivity was analyzed yielding global and local graph-theory metrics across 100 child-based functional nodes. We also compared local metrics between groups in frontopolar, supplementary motor, and sensorimotor cortices, regions implicated in recent neuroimaging and/or brain stimulation treatment studies in OCD.

Results—As in adults, the global metric small-worldness was significantly ($P<0.05$) lower in patients than controls, by 13.5% (%mean difference = 100%×(OCD mean – control mean)/control mean). This suggests less efficient information transfer in patients. In addition, modularity was lower in OCD (15.1%, $P<0.01$), suggesting less granular-- or differently organized-- functional brain parcellation. Higher clustering coefficients (23.9-32.4%, $P<0.05$) were observed in patients in frontopolar, supplementary motor, sensorimotor, and cortices with lower betweenness centrality (-63.6%, $P<0.01$) at one frontopolar site. These findings are consistent with more locally intensive connectivity or less interaction with other brain regions at these sites.

Limitations—Relatively large node size; relatively small sample size, comorbidities in some patients.

Conclusions—Pediatric OCD patients demonstrate aberrant global and local resting-state network connectivity topologies compared to healthy children. Local results accord with recent views of OCD as a disorder with sensorimotor component.

*Correspondence to: Joseph O'Neill, PhD, Division of Child & Adolescent Psychiatry, UCLA Semel Institute For Neuroscience, 760 Westwood Plaza #58-227A, Los Angeles, CA 90024-1759, USA. Tel.:±310 825-5709; fax:±310 206-4446. joneill@mednet.ucla.edu.

Conflict of interest: Nothing declared.

Keywords

Obsessive-compulsive disorder; fMRI graph theory; Frontal pole; Supplementary motor cortex; Sensorimotor cortex

1. Introduction

Obsessive-compulsive disorder (OCD) is a widespread and impairing psychiatric condition characterized by recurrent, intrusive, and disturbing thoughts (obsessions) and/or stereotyped recurrent actions (compulsions; APA, 2000). OCD affects 2.5-2.7% of children and adolescents (Rapoport et al., 2000; Heyman et al., 2003), negatively impacting family, school and social functioning (Piacentini et al., 2007), and quality of life (Lack et al., 2009). Neuroimaging has long associated OCD with metabolic hyperactivity (often lessening following treatment) in caudate and putamen, thalamus, anterior cingulate, and orbitofrontal cortex (Maia et al., 2008; Menzies et al., 2008). Treatment outcomes are often positive, but are unpredictable and frequently fall short of remission or even response (Knopp et al., 2013). Recently, neuroimaging has sought improved treatment through deeper insight into OCD pathophysiology by searching for dysfunction in global brain systems and in local systems outside the aforementioned cortico-striato-thalamic “classical OCD regions” (Anticevic et al., 2014; Fitzgerald et al., 2010; Milad and Rauch, 2012; Shin et al., 2014; Stern et al., 2012; Zhang et al., 2011).

Resting-state functional magnetic resonance imaging (rsfMRI) is well suited for such efforts. rsfMRI maps correlations between spontaneous fluctuations in blood oxygen level-dependent (BOLD) signals across the brain, revealing underlying global and local intrinsic connectivity networks. In frontostriatal and parietal brain, for example, rsfMRI has already detected aberrant connectivity in adult OCD (Stern et al., 2012; van den Heuvel and Hulshoff Pol, 2010). Conventionally, rsfMRI employs a seed, i.e., a preselected brain region with which the functional connectivity of all other areas of the brain is computed. From pulse-to-pulse of the fMRI scan, the correlation coefficient is calcualted between the BOLD signal in the seed and the BOLD signal in each other region. This technique is simple, sensitive, and easily interpreted (Fox and Raichle, 2007). But one disadvantage is that results are dependent on the choice of seed; in large, heterogeneous, OCD-relevant areas like prefrontal cortex or basal ganglia, it is difficult to place the seed accurately (Anticevic et al., 2014). The ability to identify netwroks and to gain insights outside the postulated seed-based framework is also limited (Buecke et al., 2013). As an alternative, graph-theory analysis of rsfMRI (Bullmore and Sporns, 2009) has aroused great recent interest for its capacity to quantify the topology of normal and abnormal intrinsic connectivity networks. Graph theory divides a rsfMRI dataset into a mesh of “nodes” and “edges”. Each node is a discrete volume-of-interest centered in a fixed neuroanatomic region. Each edge is a connection between two nodes that represents the strength of the time-correlation between their BOLD activities during fMRI acquisition. From the number and pattern of edges acroos the nodes, one calculates various graph-theory metrics that characterize the interconnectedness of the entire network, as well as how individual nodes interact with the rest of the brain. These higher-level metrics may be sensitive to effects not detected by seed-based methods. Graph

theory results are independent of the seed and display effects across multiple networks simultaneously (Anticevic et al., 2014). Graph theory particularly identifies isolated regions disconnected from the rest of the brain, as well as highly interconnected network “hub” regions (Dosenbach et al., 2007). Thus, graph theory affords novel opportunity to detect prospective functional abnormalities in OCD at the global brain level, as well as at nodes inside or outside classical OCD regions.

Only three previous graph-theory studies of OCD, both in adults, and only two rsfMRI studies of pediatric OCD, both non-graph theory, are reported. The first adult study (Zhang et al., 2011) identified below-normal small-world architecture in OCD in widespread “top-down control networks”, as well as local connectivity effects in multiple regions (posterior temporal cortex, middle cingulate, precuneus, thalamus, and cerebellum). The second study (Shin et al., 2014), among other results, found below-normal values of the global graph-theory parameters small-worldness and clustering coefficient in OCD. A third global parameter, modularity, was (non-significantly) lower in OCD patients than controls. Small-worldness and modularity increased in patients after treatment with selective serotonin-reuptake inhibitors (SRIs). A fourth global parameter, global efficiency, did not differ at all between patients and controls and did not respond to treatment. Patients with OCD further showed lower values of the local parameter node degree at sites in the default-mode, sensorimotor, occipital, and cingulo-opercular resting-state networks. The third study (Hou et al., 2014), alongside abnormally strengthened functional connectivity within cortico-striato-thalamic circuits, detected diminished connectivity in occipital, temporal and and cerebellar cortex in OCD. Thus, all three studies reported abnormal global network topology and effects outside classical regions in adult OCD. These findings cannot be unreservedly extrapolated to pediatric OCD since resting-state connectivity differs between children and adults even in normals (Pang et al., 2009; Lopez-Larson et al., 2011). Clinically, pediatric OCD also differs from adult OCD (Geller et al., 1998; Rosario-Campos et al., 2001; Geller, 2006). It is, for example, more familial, more common in males, more often comorbid with tic disorders, and less responsive to clomipramine (Maia et al., 2008). In pediatric OCD, one task-based fMRI study co-analyzed within-task rest periods and found below-normal connectivity between ventral medial prefrontal and posterior cingulate cortices (Fitzgerald et al., 2010). A subsequent dedicated resting-state study found below-normal connectivity between caudate and pregenual anterior cingulate in OCD (Fitzgerald et al., 2011). Thus, adult and child OCD rsfMRI investigations have observed global effects, as well as local effects inside and outside classical OCD regions.

The first objective of the present study was an exploratory comparison of global functional brain networks in children with OCD to those in healthy children, using rsfMRI graph theory. Drawing on Shin et al. (2014), we examined the global metrics small-worldness, modularity, and global efficiency and anticipated effects of OCD on the first two, but not the third. (Clustering coefficient in our study was observed on the local, rather than global, level, see below.) Given that small-worldness and modularity, but not global efficiency, responded in that study to SRIs and that these dugs typically reduce OCD symptoms, we additionally correlated these endpoints against severity of OCD symptoms on the Children's Yale-Brown Obsessive-Compulsive Scale (CY-BOCS; Scahill et al., 1997).

Our second objective was to compare local graph theory measures in children with OCD to those in healthy children. We first examined a targeted group of non-classical brain regions that have been less explored in OCD, where, however, effects of OCD had been documented in multiple studies. As non-classical regions, we chose the frontal poles, supplementary motor cortex, and sensorimotor cortex (precentral plus postcentral gyri). The frontal poles have only recently emerged as potential sites of abnormality in OCD, yet already numerous studies with single-photon emission correlated tomography (SPECT; Yamanishi et al., 2009), positron emission tomography (PET; Saxena et al., 2002), volumetric or surface-based structural MRI (Huyser et al., 2013; Szeszko et al., 2008; Venkatasubramanian et al., 2012), task-based fMRI (Milad et al., 2013; Viard et al., 2005), and rsfMRI (Cheng et al., 2013; Fitzgerald et al., 2011; Meunier et al., 2012; Stern et al., 2012) localize effects of OCD to frontopolar cortex. fMRI has found abnormal activation in post-central (Nakao et al., 2009) and supplementary motor cortices (Yücel et al., 2007) in OCD, and in precentral cortex in unaffected first-degree relatives of OCD patients (Hou et al., 2014). Moreover, transcranial magnetic stimulation (TMS) studies indicate primary or secondary involvement of supplementary motor and sensorimotor cortex (Greenberg et al., 2000; Mantovani et al., 2006, 2010; Richter et al. 2012; reviewed in Bunse et al., 2014) in OCD; while two controlled trials found that TMS can remediate OCD symptoms (Mantovani et al., 2013; Russo et al., 2014). In addition, Shin et al. (2014) observed that, subsequent to SRI treatment, OCD patients manifested abnormal connectivity in sensorimotor regions. Abnormal EEG power has also been observed in OCD patients during and preceding voluntary movement in supplementary motor and sensorimotor cortex (Leocani et al., 2001). Thus, there was reasonable expectation of finding effects of pediatric OCD in these regions with graph theory and rsfMRI. For comparison, we analyzed a second group of classical cortico-striatal OCD regions, including caudate, orbitofrontal cortex, and anterior midcingulate cortex. Finally, we tested a third group consisting of the rest of the brain: regions where we had limited anticipation of effects of OCD.

Among the numerous local graph-theory metrics, we chose the clustering coefficient as our probe for possible effects of OCD on connectivity at each node. A high clustering coefficient results from dense local connections; a low clustering coefficient reflects a sparsely interconnected nodal neighborhood, one more populated with remote connections. To complement the clustering coefficient, we calculated a second metric, betweenness centrality, at each node. High betweenness centrality denotes a node through which the shortest paths between many other (not just neighboring) node pairs pass. To first-order approximation, high betweenness centrality identifies nodes that are candidate brain network hubs, implying appreciable non-local functional connectivity. (Superior hub identification is achieved with more sophisticated methods; Guimerà et al. 2007, Sporns et al. 2007.) We measured clustering coefficient and betweenness centrality during resting-state at nodes in all three groups of brain regions to determine whether hub character or more local character predominated, in children with OCD compared to those without OCD.

2. Methods

2.1. Participants

Twenty-one children with DSM-IV (APA, 2000) OCD and 20 age- and sex-matched healthy controls participated (Table 1). All were right-handed. Subjects were recruited by referral from UCLA clinics and local psychiatrists and pediatricians, as well as through flyers, radio, and Internet advertisements. Children in the patient group had to exhibit CY-BOCS Total Score ≥16, indicating clinically significant OCD symptoms. Subjects were also administered the Kiddie Schedule for Affective Disorders and Schizophrenia (K-SADS; Kaufman et al., 1997) to identify any comorbid disorders. Subjects were excluded if they met diagnostic criteria for schizophrenia, schizoaffective disorder, bipolar disorder, or if OCD was not their primary diagnosis. Healthy controls were excluded if they met criteria for any Axis I disorder. Full-scale IQ<80 on the Wechsler Abbreviated Scale of Intelligence (WASI; Wechsler, 1999) was exclusionary. rsfMRI data from 4 OCD subjects were excluded due to excessive head motion during scanning. These subjects were excluded if ≥75 images were discarded due to motion. This was done so as to preserve at least 5 min of usable BOLD data, a minimum acceptable time-span for sampling the human resting state (Birn et al., 2013; Van Dijk et al., 2010). All participants provided written informed consent/assent and the study was approved by the UCLA Institutional Review Board. Data reported here were collected at baseline as part of a larger study examining the neurophysiologic correlates of cognitive behavioral therapy for pediatric OCD.

2.2. Resting-state fMRI acquisition

All magnetic resonance data were acquired at 3 T using a Siemens Trio with 12-channel phased-array headcoil. Whole-brain fMRI was collected using an 8-min echo-planar imaging sequence (repetition-time/echo-time=2000/30 ms, flip angle=75°, voxels $3.4\times3.4\times4.0$ mm^3, 1-mm interslice gap). Subjects were instructed to rest with eyes closed, to remain as still as possible, and not to sleep. High-resolution T1-weighted whole-brain structural MRI for offline co-registration of BOLD data was acquired using an axial magnetization-prepared rapid gradient-echo sequence (repetition-time/echo-time= 1900/3.26 ms, voxels $1\times1\times1$ mm^3).

2.3. Resting-state fMRI processing

Functional data were preprocessed using FMRI Software Library 5.0.4 (http://www.fmrib.ox.ac.uk/fsl; Smith et al., 2004). To allow magnetization equilibrium, we discarded the first 4 images. Data were slice-time corrected and motion-corrected (using the Motion-corrected Linear Image Registration Tool--McFLIRT) prior to band-pass filtering (0.009-0.08 Hz). A 7 degrees-of-freedom transform was used to register each subject's functional image to the T1-weighted structural MRI, and a 12 degrees-of-freedom transform was used to register the structural MRI to Montréal Neurological Institute (MNI) standard brain atlas space. Although the MNI is an adult template, it was used since there is no accepted child standard in the field. All images were inspected for proper registration to the MNI template. Data were then resampled to 4-mm space. White matter, cerebrospinal fluid, and temporal derivatives were removed by linear regression. The white-matter mask was eroded prior to extracting time-series for denoising. Motion scrubbing was used to remove

time points with either framewise displacement (FD) >2 mm or derivative of root mean squared variance over voxels (DVARS>25%; Power et al., 2012). Mean FD and DVARS were compared between groups. One hundred functional nodes (Fig. 1) were generated per Craddock et al. (2012) via spatially constrained spectral clustering of an age-equivalent typically developing child functional dataset, the NKI (Nathan Kline Institute for Psychiatric Research) normal child brain set in the ADHD-200 Global Competition Dataset (Brown et al., 2012). Anatomical localization of nodes was determined using the Harvard–Oxford cortical and subcortical probabilistic atlases supplied with the FMRI Software Library. The choice of 100 nodes represented a compromise between obtaining adequate brain coverage and resolution while avoiding oversampling, given our 240 excitations per scan. Applying these nodes to each individual's rsfMRI time-series data, all pairwise Pearson correlation coefficients between nodes were calculated. From this, we derived binarized (based on a range of sparsities, see below), undirected graphs, or functional connectivity matrices, for each subject.

2.4. Graph Theory

Graph-theory metrics were calculated using Matlab Brain Connectivity Toolbox (www.brain-connectivity-toolbox.net; Rubinov and Sporns, 2010). Global measures derived included small-worldness, modularity, and global efficiency. High small-worldness implies a highly effective topological organization that combines regional specialization and efficient global information transfer (Watts and Strogatz, 1998; Latora and Manchiori, 2003; Bassett et al., 2011). Small-world architecture resembles, for example, a municipal subway system, where there are local trains making numerous local stops, combined with express trains with fewer, more remote stops. Small-worldness was calculated (Bassett et al., 2011; Humphries and Gurney, 2008) as the ratio of the global clustering coefficient of the actual brain network to the clustering coefficient of a random network divided by the ratio of the characteristic pathlength (minimum node-to-node distance counted in edges) of the real brain network to the pathlength of a random network.

Modularity is a community-structure metric (Newman and Girvan, 2004; Meunier et al., 2009). A module is a subset of nodes more densely connected to each other than to outside nodes (Radicchi et al., 2004). Optimal modularity (Scholl and Leslie, 1999) implies an ideal number of communities in the network (Telesford et al., 2011). Global efficiency is the average inverse path length of the shortest paths connecting all nodes in a network (Gong et al., 2009). High global efficiency implies that nodes throughout the network are on average relatively close together topologically.

Local measures included clustering coefficient and betweenness centrality. The clustering coefficient (Watts and Strogatz, 1998; Bullmore and Sporns, 2009; Braun et al., 2012) is the number of actual connections between the nearest neighbors of a node divided by the maximum possible number of such connections. High clustering coefficients characterize complex, as opposed to random, networks; signal high likelihood of neighboring (short) connections (Guye et al., 2010; van den Heuvel and Hulshof Pol, 2010); and usually accompany efficient and robust local information transfer (He and Evans, 2010; Bassett et al., 2011). High betweenness centrality (Freeman, 1978; Newman, 2006), in contrast,

describes a node that is traversed by the shortest path interconnecting many (not just neighboring) node pairs. In coarse approximation, high betweenness centrality signifies hub nodes in a network (He et al., 2008), although more sophisticated metrics, such as motif fingerprints, detect and classify hubs more accurately (Guimerà et al., 2007; Sporns et al., 2007).

Graph-theory metrics were calculated at sparsities ranging from 10%-20% of the strongest connections within the connectivity matrix. Area-under-the-curve (AUC) was calculated for each metric across all values of sparsity in 1% intervals. These AUC values were used for statistical comparisons.

2.5. Statistical analyses

A few local graph-theory endpoints had non-normal distributions, as evidenced by a correlation coefficient on normal quantile plots exceeding the critical value of 0.950 for the control or 0.952 for the OCD sample. These endpoints included the clustering coefficient at one node and betweenness centrality at four nodes (Table 3). Data for these endpoints were rank-transformed to enable non-parametric testing. Parametric testing was used for local metrics at the other nodes, the global metrics, and the clinical and demographic variables, which had normal distributions. An omnibus approach was taken to multiple comparisons of global measures. Multivariate analysis-of-variance was performed to test for effects of diagnosis across the three global measures small-worldness, modularity, and global efficiency. For a significant multivariate finding, mean values for the two groups were subsequently compared for each metric using two-sided post-hoc protected T-tests.

Regarding local graph-theory indices, to leverage a priori expectations of diagnosis at several target sites, whilst exercising due control for multiple comparisons, the following statistical testing strategy was adopted. Mean values of clustering coefficient and betweenness centrality for the OCD and healthy control samples were compared with two-sided T-test at each node using false discovery rate (FDR) correction for multiple comparisons. The nodes were divided into three groups and FDR was performed within each group. As described above, the first group (Table 3) comprised nodes in less explored non-classical OCD brain regions where we had a priori expectations of effects of OCD. This group (Fig. 1) included 5 nodes in sensorimotor cortex, 1 in midline (i.e., left+right) supplementary motor cortex, and 10 in frontopolar cortex for a total of 16. The second group (Table 4) comprised nodes in well-explored classical OCD regions where effects of OCD were again expected. This group included 2 nodes in the caudate, 3 in orbitofrontal cortex, and 3 in anterior cingulate cortex, for 8 nodes total. The third group comprised all other nodes in the brain (77).

Given findings in adult OCD that small-worldness and modularity (but not global efficiency) increased after treatment (Shin et al., 2014) while severity of OCD symptoms usually decreases after treatment, a robust linear model was used to test exploratory correlations between AUCs for the three global graph-theory metrics and CY-BOCS Obsession and Compulsion subscores, as well as Total Score. Significance was thresholded at $P<0.05$ for all tests.

3. Results

3.1. Demographic and clinical characteristics

Participant characteristics are summarized in Table 1. The two subject groups did not differ significantly in numbers of boys and girls or age. Of the 21 OCD subjects, 18 were unmedicated and 2 had been on a stable dose of SRIs for the preceding 12 weeks and remained so throughout the study. The one remaining subject had been prescribed stimulant medication, but was asked to refrain from taking it the day of the scan. Fifteen OCD subjects met criteria for one or more comorbid disorders (generalized anxiety disorder 6, attention deficit hyperactivity disorder 4, social phobia 4, oppositional defiant disorder 2, separation anxiety disorder 2, specific phobia 2, Tourette's syndrome 2, transient tic disorder 1, tic disorder NOS 1, depressive disorder NOS 1, dysthymic disorder 1).

3.2. BOLD Data Quality

Subject head motion pre-scrubbing, quantified by mean framewise displacement (OCD 0.16±0.09 mm, Control 0.13±0.04 mm; $P>0.10$) and DVARS (OCD 29.2±3.0, Control 28.5±3.1; $P>0.10$) did not differ significantly between the groups. In matrix form, Fig. 2 depicts r-values for correlations between all possible two-way combinations of the 100 Craddock nodes. Values were calculated across the rsfMRI BOLD acquisition epoch and averaged across the pediatric OCD and healthy control groups. Higher correlation between anatomically neighboring nodes imparts a degree of modular structure to the correlation matrices. Also shown are histograms for the r-values for the two groups, which were normal and highly overlapping. These quality control results imply that the effects of diagnosis on global and local graph-theory metrics reported below were not influenced by between-group differences in head motion.

3.3. Global Measures

Multivariate analysis-of-variance for the measures small-worldness, modularity, and global efficiency evinced a significant between-subjects effect of Diagnosis ($F(3, 37)=3.6$, $P< 0.05$; Fig. 3). In post-hoc protected tests, OCD patients exhibited significantly ($P<0.05$) lower small-worldness (-13.5%, %difference = 100%×(OCD group-mean – control group-mean)/ control group-mean) and modularity (-15.1%, $P<0.01$) than controls (Table 2). No significant between-group differences in global efficiency were evident ($P=0.890$). These findings are all consistent with prior research (Shin et al., 2014). Note that small-worldness in the present study is expressed as AUC, and therefore may be larger than small-worldness in other studies measured at single values of sparsity. Our small-worldness endpoint assayed at single sparsities ranged 1.4-2.1 (Fig. 3). This overlaps partially with the 1.1-1.9 range in Fornito et al. (2010). Within the OCD sample, small-worldness was significantly positively correlated with CY-BOCS Obsessions subscore (Spearman $r=0.56$, $P=0.008$; Fig. 3). Modularity and global efficiency did not correlate significantly with any CY-BOCS scores.

3.4. Local Measures

The local graph-theory metrics clustering coefficient and betweenness centrality are listed for first-group nodes in Table 3 and for second-group nodes in Table 4. In FDR-corrected T-

tests in the first node group, mean clustering coefficient was significantly higher for OCD patients than for controls at 1 site in left sensorimotor cortex (Node 100; 25.0%, P<0.01), in the sole midline supplementary motor cortex site (Node 88; 25.8%, P<0.01), and at 2 left (Nodes 56 23.9%, P<0.05; Node 80 27.8%, P<0.01) and 1 right (Node 66 32.4%, P<0.01) frontopolar cortex sites. Betweenness centrality, which had high standard deviations (Table 3), was significantly lower for patients at Node 56 only (-63.6%, P<0.01). After FDR correction, there were no significant between-group differences in clustering coefficient and betweenness centrality at any second-group or third-group nodes (all P>0.05). Thus, there were notable bilateral elevated clustering coefficient (Fig. 4) and reduced betweenness centrality in frontopolar cortex in the pediatric OCD sample.

4. Discussion

In this exploratory resting-state fMRI brain network analysis of pediatric OCD using graph theory, we found lower small-worldness and modularity compared with healthy controls. These global metrics are consistent with suboptimal network architecture during the resting state in pediatric OCD. In addition, we found local network abnormalities in three brain areas: frontal pole, supplementary motor cortex, and sensorimotor cortex, structures implicated in prior neuroimaging and/or therapeutic TMS studies of OCD. We did not find significant local effects elsewhere in the brain, including in “classical” cortico-striatal OCD regions. In concert, these findings support the idea of aberrant cognitive motor and sensorimotor functional organization in OCD. They may represent generally abnormal connectivity patterns that are also detectable in the resting state.

Global findings comprised below-normal small-worldness and modularity in OCD alongside normal global efficiency. This replicates adult OCD findings (Zhang et al., 2011; Shin et al., 2014) of significantly lower small-worldness, lower but not significantly lower modularity, and equal global efficiency in patients vs. healthy controls. Small-world networking is a highly effective topological organization that combines regional specialization and efficient global information transfer (Watts and Strogatz, 1998; Latora and Manchiori, 2003; Bassett et al., 2011). Optimal modularity (Scholl and Leslie, 1999) implies an ideal number of communities in a network (Telesford et al., 2011). The below-normal values of these two parameters in our OCD sample point to less effectual neurofunctional connectivity in children with OCD during the resting-state. Low modularity is consistent with sparsity of modules and relative over-connectedness of certain nodes, diminishing the ability of the network to adapt (Guye et al., 2010). Rather than too few modules, lower modularity in OCD may alternatively reflect a different modular scheme (i.e., different node membership in the same number of modules) than normal. No significant effects of group were observed for global efficiency in our study (nor in Shin et al., 2014). Perhaps this metric is not sensitive to features of network topology impinged on by OCD.

Within the OCD group, small-worldness correlated positively with OCD obsessions. I.e., patients with higher small-worldness had more severe obsessive symptoms, even though, as a group, small-worldness was lower for OCD than for control subjects. This was furthermore puzzling since small-worldness in Shin et al. (2014) increased after adult patients were treated with SRIs. One explanation could be that the OCD brain favors low small-worldness

and departure from this state aggravates symptoms; but after SRI treatment the brain shifts to a new state of higher small-worldness and lower symptoms. This finding requires replication.

In supplementary motor and sensorimotor cortices we found higher clustering coefficient in OCD patients than in controls. The localization of these findings is in harmony with recent TMS studies (reviewed in Russo et al., 2014) uncovering elevated cortical excitability and dysfunction in sensorimotor integration in OCD, with encouraging trials of supplementary motor cortex TMS as a therapy for OCD, and with an emerging perspective on OCD as a "sensorimotor" condition akin to Tourette's syndrome and more frank movement disorders (Mantovani et al., 2013; Russo et al., 2014). Elevated clustering coefficient indicates denser internal networking in these regions in OCD than in healthy children. Such internal networking could promote local cortical excitability and/or impair the putative role of these brain areas in modulatory inhibition of hyperactive cortico-striatal OCD citcuits (Mantovani et al., 2013).

Our strongest local effects were registered at the frontal pole where we found elevated clustering coefficient, alongside (at one site) diminished betweenness centrality. This was similar to Meunier et al. (2012) who observed lower nodal connectivity—indicating weaker connection with the rest of the brain—in adult OCD patients than in controls in frontal pole. The frontal pole has only recently been implicated in OCD but there are numerous OCD-related findings there with diverse imaging modalities (Yamanishi et al., 2009; Saxenea et al., 2002; Huyser et al., 2013; Szeszko et al., 2008; Venkatasubramanian et al., 2012; Milad et al., 2013; Viard et al., 2005), including rsfMRI (Cheng et al., 2013; Fitzgerald et al., 2011; Meunier et al., 2012; Stern et al., 2012). Our present graph-theory results further document abnormal functional connectivity of this structure in pediatric OCD. Frontopolar cortex is associated with decision-making, concurrently entertaining two possibilities in mind, and protecting planned behaviors against distraction (Koechlin and Hyafil, 2007). There is moderate evidence of impaired decision-making (Sachdev and Mahli, 2005), impaired divided attention (Chang et al., 2007; Moritz et al., 2006), and elevated distractibility (van den Heuvel et al., 2005) in OCD. As mentioned, a high clustering coefficient usually accompanies efficient and robust local information transfer (He and Evans, 2010; Bassett et al., 2011). High betweenness centrality, in contrast, is significantly increased by interconnections with non-local nodes (Zalesky et al., 2010). Thus, the frontal pole in OCD may act more autonomously, being partly insulated from modulation by other brain regions (and/or may act less to modulate other regions). Such a local network topology could lengthen the timescale of the execution of frontopolar cognitive functions, which could be described as "cognitive motor" since they impact moment-to-moment selection of which motor actions to initiate, which to continue, and which to decease. Consequences could include indecision, perpetual holding of multiple possibilities in mind, and overly rigid adherence to behavioral intent (e.g., compulsive behaviors). Further effects could include difficulty shifting between tasks and difficulty restoring attention to its original focus, after it is pulled away by a distractor. The frontal pole represents a possible target for TMS or other neurostimulatory investigative interventions for OCD, as contemplated for major depression and motor disorders (Triggs et al., 1999; Lang et al., 2005; Manuel et al., 2014).

After correction for multiple comparisons, we failed to find significant effects of OCD on local graph-theory metrics in classical OCD brain regions (orbitofrontal cortex, caudate, anterior cingulate cortex). One possible explanation be that classic OCD pathophysiology involving cortico-striatal loops represents functional hyperactivity within an essentially normal network architecture. I.e., not bad wiring, but too much current in the wires. OCD-related disturbances in cortices outside the core regions may manifest instead as aberrant network organization, which rsfMRI graph-theory methodology is better designed to pick-up.

A limitation of this study is the size of our nodes. Smaller nodes may have yielded greater regional specificity. Another limitation is sample size (20-21 subjects per group). Nonetheless, our global graph-theory results are consistent with prior rsfMRI work in OCD, and our local findings are anatomically concordant with earlier neuroimaging results. Some patients suffered from psychiatric comorbidities, which could themselves influence graph-theory endpoints. Comorbidities are very common in OCD rendering it difficult to recruit exclusively patients with pure OCD in clinical samples, which would themselves be somewhat less representative of typical clinical cases.

In sum, global graph-theory metrics in this rsfMRI investigation yield evidence for less efficient global network connectivity in children with OCD than in healthy children. In addition, local network organization in the resting-state in pediatric OCD entails higher internal functional connectivity in sensorimotor, supplementary motor, and frontal polar cortex.

Acknowledgments

Role of funding source: This work was supported by grants from the National Institute of Mental Health R01MH081864 (JON, JCP) and R01MH085900 (JON, JDF).

References

APA. Diagnostic and Statistical Manual of Mental Disorders (DSM-IV-TR). American Psychiatric Association; Washington, DC: 2000.

Anticevic A, Hu S, Zhang S, Savic A, Billingslea E, Wasylink S, Repovs G, Cole MW, Bednarski S, Krystal JH, Bloch MH, Li CSR, Pittenger C. Global resting-state functional magnetic resonance imaging analysis identifies frontal cortex, striatal, and cerebellar dysconnectivity in obsessive-compulsive disorder. Biol Psychiatry. 2014; 75:595–605. [PubMed: 24314349]

Bassett DS, Brown JA, Deshpande V, Carlson JM, Grafton ST. Conserved and variable architecture of human white matter connectivity. NeuroImage. 2011; 54(2):1262–1279. [PubMed: 20850551]

Beucke JC, Sepulcre J, Talukdar T, Linnman C, Zschenderlein K, Endrass T, Kaufmann C, Kathmann N. Abnormally high degree connectivity of the orbitofrontal cortex in obsessive-compulsive disorder. JAMA Psychiatry. 2013; 70(6):619–629. [PubMed: 23740050]

Birn RM, Molloy EK, Patriat R, Parker T, Meier T, Kirk GR, Nair VA, Meyerand ME, Prabhakaran V. The effect of scan length on the reliability of resting-state fMRI connectivity estimates. NeuroImage. 2013; 83:550–558. [PubMed: 23747458]

Braun U, Plichta MM, Esslinger C, Sauer C, Haddad L, Grimm O, Mier D, Mohnke S, Heinz A, Erk S, Walter H, Seiferth N, Kirsch P, Meyer-Lindenberg A. Test-retest reliability of resting-state connectivity network characteristics using fMRI and graph theoretical measures. Neuroimage. 2012; 59(2):1404–1412. [PubMed: 21888983]

Brown MRG, Sidhu GS, Greiner R, Asgarian N, Bastani M, Silverstone PH, Greenshaw PH, Dursun SM. ADHD-200 Global Competition: diagnosing ADHD using personal characteristic data can outperform resting state fMRI measurements. Fron Systems Neurosci. 2012; 6(69)doi: 10.3389/fnsys.2012.00069

Bullmore E, Sporns O. Complex brain networks: graph theoretical analysis of structural and functional systems. Nat Rev Neurosci. 2009; 10(3):186–198. [PubMed: 19190637]

Bunse T, Wobrock T, Strube W, Padberg F, Palm U, Falkai P, Hasan A. Motor cortical excitability assessed by transcranial magnetic stimulation in psychiatric disorders: A systematic review. Brain Stim. 2014; 7:158–169.

Chang SW, McCracken JT, Piacentini JC. Neurocognitive correlates of child obsessive compulsive disorder and Tourette syndrome. J Clin Exp Neuropsych. 2007; 29(7):724–733.

Cheng Y, Xu J, Nie B, Luo C, Yang T, Li H, Lu J, Xu L, Shan B, Xu X. Abnormal resting-state activities and functional connectivities of the anterior and the posterior cortexes in medication-naïve patients with obsessive-compulsive disorder. PLos One. 2013; 8(6):e67478. [PubMed: 23840714]

Craddock RC, James GA, Holtzheimer PE III, Hu XP, Mayberg HS. A whole brain fMRI atlas generated via spatially constrained spectral clustering. Hum Brain Mapping. 2012; 33(8):1914–1928.

Dosenbach NUF, Fair DA, Miezin FM, Cohen AL, Wenger KK, Dosenbach RAT, Fox MD, Snyder AZ, Vincent JL, Raichle ME, Schlaggar BL, Petersen SE. Distinct brain networks for adaptive and stable task control in humans. PNAS. 2007; 104(26):11073–11078. [PubMed: 17576922]

Fitzgerald KD, Stern ER, Angstadt M, Nicholson-Muth KC, Maynor MR, Welsh RC, Hanna GL, Taylor SF. Altered function and connectivity of the medial frontal cortex in pediatric obsessive-compulsive disorder. Biol Psychiatry. 2010; 68(11):1039–1047. [PubMed: 20947065]

Fitzgerald KD, Welsh RC, Stern ER, Angstadt M, Hanna GL, Abelson JL, Taylor SF. Developmental alterations of frontal-striatal-thalamic connectivity in obsessive-compulsive disorder. J Am Acad Child Adol Psychiatry. 2011; 50(9):938–948.

Fornito A, Zalesky A, Bullmore ET. Network scaling effects in graph analytic studies of human resting-state fMRI data. Fron System Neurosci. 2010; 4(22)doi: 10.3389/fnsys.2010.00022

Fox MD, Raichle ME. Spontaneous fluctuations in brain activity observed with functional magnetic resonance imaging. Nat Rev Neurosci. 2007; 8:700–711. [PubMed: 17704812]

Freeman LC. Centrality in social networks conceptual clarification. Soc Networks. 1978/1979; 1:215–239.

Geller DA. Obsessive-compulsive and spectrum disorders in children and adolescents. Psychiat Clin N Am. 2006; 29(2):353–370.

Geller DA, Biederman J, Jones J, Shapiro S, Schwartz S, Park KS. Obsessive-compulsive disorder in children and adolescents: A review. Harv Rev Psychiat. 1998; 5(5):260–273.

Gong G, Rosa-Neto P, Carbonell F, Chen ZJ, He Y, Evans AC. Age- and gender-related differences in the cortical anatomical network. J Neurosci. 2009; 29(50):15684–15693. [PubMed: 20016083]

Greenberg BD, Ziemann U, Corá-Locatelli G, Harmon A, Murphy DL, Keel JC, Wassermann EM. Altered cortical excitability in obsessive-compulsive disorder. Neurology. 2000; 54(1):142–147. [PubMed: 10636140]

Guimerà R, Sales-Pardo M, Amaral LAN. Classes of complex networks defined by role-to-role connectivity profiles. Nat Phys. 2007; 3(1):63–69. [PubMed: 18618010]

Guye M, Bettus G, Bartolomei F, Cozzone PJ. Graph theoretical analysis of structural and functional connectivity MRI in normal and pathological brain networks. Magma. 2010; 23(5-6):409–421. [PubMed: 20349109]

He Y, Chen Z, Evans A. Structural insights into aberrant topological patterns of large-scale cortical networks in Alzheimer's Disease. J Neuroscl. 2008; 28(18):4756–4766.

He Y, Evans A. Graph theoretical modeling of brain connectivity. Curr Opin Neurol. 2010; 23(4):341–350. [PubMed: 20581686]

Heyman I, Fombonne E, Simmons H, Ford T, Meltzer H, Goodman R. Prevalence of obsessive-compulsive disorder in the British nationwide survey of child mental health. Int Rev Psychiatry. 2003; 15(1-2):178–184. [PubMed: 12745330]

Hou JM, Zhao M, Zhang W, Song LH, Wu WJ, Wang J, Zhou DQ, Xie B, He M, Guo JW, Qu W, Li HT. Resting-state functional connectivity abnormalities in patients with obsessive–compulsive disorder and their healthy first-degree relatives. J Psychiatry Neurosci. 2014; 39(5):304–311. [PubMed: 24866415]

Humphries MD, Gurney K. Network 'small-world-ness': A quantitative method for determining canonical network equivalence. PLoS One. 2008; 3(4):e0002051. [PubMed: 18446219]

Huyser C, van den Heuvel OA, Wolters LH, de Haan E, Boer F, Veltman DJ. Increased orbital frontal gray matter volume after cognitive behavioural therapy in paediatric obsessive compulsive disorder. World J Biol Psychiatry. 2013; 14(4):319–331. [PubMed: 22746998]

Kaufman J, Birmaher B, Brent D, Rao U, Flynn C, Moreci P, Williamson D, Ryan N. Schedule for Affective Disorders and Schizophrenia for School-Age Children-Present and Lifetime Version (K-SADS-PL): initial reliability and validity data. J Am Acad Child Adolesc Psychiatry. 1997; 36(7): 980–988. [PubMed: 9204677]

Knopp J, Knowles S, Bee P, Lovell K, Bower P. A systematic review of predictors and moderators of response to psychological therapies in OCD: Do we have enough empirical evidence to target treatment? Clin Psychol Rev. 2013; 33(8):1067–1081. [PubMed: 24077387]

Koechlin E, Hyafil A. Anterior prefrontal function and the limits of human decision-making. Science. 2007; 318(5850):594–598. [PubMed: 17962551]

Lack CW, Storch EA, Keeley ML, Gefken GR, Ricketts ED, Murphy TK, Goodman WK. Quality of life in children and adolescents with obsessive-compulsive disorder: base rates, parent-child agreement, and clinical correlates. Soc Psychiatry Psychiatric Epidemiol. 2009; 44(11):935–942.

Lang N, Siebner HR, Ward NS, Lee L, Nitsche MA, Paulus W, Rothwell JC, Lemon RN, Frackowiak RS. How does transcranial DC stimulation of the primary motor cortex alter regional neuronal activity in the human brain? Eur J Neurosci. 2005; 22:495–504. [PubMed: 16045502]

Latora V, Marchiori M. Economic small-world behavior in weighted networks. Eur Phys J B. 2003; 32:249–263.

Leocani L, Locatelli M, Bellodi L, Fornara C, Hénin M, Magnani G, Mennea S, Comi G. Abnormal pattern of cortical activation associated with voluntary movement in obsessive-compulsive disorder: An EEG study. Am J Psychiatry. 2001; 158:140–142. [PubMed: 11136650]

Lopez-Larson MP, Anderson JS, Ferguson MA, Yurgelun-Todd D. Local brain connectivity and associations with gender and age. Devel Cog Neurosci. 2011; 1(2):187–197.

Maia TV, Cooney RE, Peterson BS. The neural bases of obsessive-compulsive disorder in children and adults. Development Psychopathol. 2008; 20(4):1251–1283.

Mantovani A, Lisanby SH, Pieraccini F, Ulibelli M, Castrogiovanni P, Rossi S. Repetitive transcranial magnetic stimulation (rTMS) in the treatment of obsessive-compulsive disorder (OCD) and Tourette's syndrome (TS). Int J Neuropsychopharmacol. 2006; 9:95–100. [PubMed: 15982444]

Mantovani A, Rossi S, Bassi BD, Simpson HB, Fallon BA, Lisanby SH. Modulation of motor cortex excitability in obsessive-compulsive disorder: an exploratory study on the relations of neurophysiology measures with clinical outcome. Psychiatry Res. 2013; 210(3):1026–1032. [PubMed: 24064461]

Mantovani A, Simpson HB, Fallon BA, Rossi S, Lisanby SH. Randomized sham-controlled transcranial magnetic stimulation in treatment-resistant obsessive-compulsive disorder. Int J Neuropsychopharmacol. 2010; 13:217–227. [PubMed: 19691873]

Manuel AL, David AW, Bikson M, Schinder A. Frontal TDCS modulates orbitofrontal reality filtering. Neuroscience. 2014; 265:21–27. [PubMed: 24508152]

Menzies L, Chamberlain SR, Laird AR, Thelen SM, Sahakian BJ, Bullmore ET. Integrating evidence from neuroimaging and neuropsychological studies of obsessive-compulsive disorder: the orbitofronto-striatal model revisited. Neurosci Biobehav Rev. 2008; 32(3):525–549. [PubMed: 18061263]

Meunier D, Achard S, Morcom A, Bullmore E. Age-related changes in modular organization of human brain functional networks. Neuroimage. 2009; 44(3):715–723. [PubMed: 19027073]

Meunier D, Ersche KD, Craig KJ, Fornito A, Merlo-Pich E, Fineberg NA, Shabbir SS, Robbins TW, Bullmore ET. Brain functional connectivity in stimulant drug dependence and obsessive-compulsive disorder. Neuroimage. 2012; 59:1461–1468. [PubMed: 21871569]

Milad MR, Rauch SL. Obsessive-compulsive disorder: beyond segregated cortico-striatal pathways. Trends Cog Sciences. 2012; 16(1):43–51.

Moritz S, Kuelz AK, Jaconsen D, Kloss M, Fricke S. Severity of subjective cognitive impairment in patients with obsessive-compulsive disorder and depression. Anx Disord. 2006; 20:427–443.

Nakao T, Nakagawa A, Nakatani E, Nabeyama M, Sanematsu H, Yoshiura T, Togao O, Tomita M, Masuda Y, Yoshioka K, Kuroki T, Kanba S. Working memory dysfunction in obsessive-compulsive disorder: A neuropsychological and functional MRI study. J Psychiatr Res. 2009; 43:784–791. [PubMed: 19081580]

Newman ME. Modularity and community structure in networks. Proc Natl Acad Sci USA. 2006; 103(23):8577–8582. [PubMed: 16723398]

Newman ME, Girvan M. Finding and evaluating community structure in networks. Physical Rev E: Statistical, Nonlinear, and Soft Matter Physics. 2004; 69(2 Pt 2):026113.

Pang GF, Wang SH, Ren YL, Ma L, Chen J, Xing W, Dong X. Cognitive development of normal school age children: a resting-state fMRI study. Zhonghua Yi Xue Za Zhi. 2009; 89(19):1313–1317. [PubMed: 19615183]

Piacentini J, Peris TS, Bergman RL, Chang S, Jaffer M. Functional impairment in childhood OCD: development and psychometrics properties of the Child Obsessive-Compulsive Impact Scale-Revised (COIS-R). J Clin Child Adol Psychol. 2007; 36(4):645–653.

Power JD, Barnes KA, Snyder AZ, Schlaggar BL, Petersen SE. Spurious but systematic correlations in functional connectivity MRI networks arise from subject motion. Neuroimage. 2012; 59(3):2142–2154. [PubMed: 22019881]

Radicchi F, Castellano C, Cecconi F, Loreto V, Parisi D. Defining and identifying communities in networks. Proc Natl Acad Sci USA. 2004; 101(9):2658–2663. [PubMed: 14981240]

Rapoport JL, Inoff-Germain G, Weissman MM, Greenwald S, Narrow WE, Jensen PS, Lahey BB, Canino G. Childhood obsessive-compulsive disorder in the NIMH MECA study: parent versus child identification of cases. Methods for the epidemiology of child and adolescent mental disorders. J Anx Disord. 2000; 14(6):535–548.

Richter MA, de Jesus DR, Hoppenbrouwers S, Daigle M, Deluce J, Ravindran LN, Fitzgerald PB, Daskalakis ZJ. Evidence for cortical inhibitory and excitatory dysfunction in obsessive compulsive disorder. Neuropsychopharmacol. 2012; 37(5):1144–1151.

Rosario-Campos MC, Leckman JF, Mercadante MT, Shavitt RG, Prado HS, Sada P, Zamignani D, Miguel EC. Adults with early-onset obsessive-compulsive disorder. Am J Psychiatry. 2001; 158(11):1899–1903. [PubMed: 11691698]

Rubinov M, Sporns O. Complex network measures of brain connectivity: Uses and interpretations. NeuroImage. 2010; 52:1059–1069. [PubMed: 19819337]

Russo M, Naro A, Mastroeni C, Morgante F, Terranova C, Muscatello MR, Zoccali R, Calabrò RS, Quartarone A. Obsessive-compulsive disorder: a “sensory-motor” problem? Int J Psychophysiol. 2014; 92(2):74–78. [PubMed: 24631627]

Sachdev PS, Malhi GS. Obsessive–compulsive behaviour: a disorder of decision-making. Aust N Z J Psychiatry. 2005; 39:757–763. [PubMed: 16168033]

Saxena S, Brody AL, Ho ML, Alborzian S, Maidment KM, Zohrabi N, Huang SC, Wu HM, Baxter LR Jr. Changes after behavior therapy among responsive and nonresponsive patients with obsessive-compulsive disorder. Arch Gen Psychiatry. 2002; 59:250–261. [PubMed: 11879163]

Scahill L, Riddle MA, McSwiggin-Hardin M, Ort SI, King RA, Goodman WK, Cicchetti D, Leckman JF. Children's Yale-Brown Obsessive Compulsive Scale: reliability and validity. J Am Acad Child Adol Psychiat. 1997; 36:844–852.

Shin DJ, Jung WH, He Y, Wang J, Shim G, Byun MS, Jang JH, Kim SN, Lee TY, Park HY, Kwon JS. The effects of pharmacological treatment on functional brain connectome in obsessive-compulsive disorder. Biol Psychiatry. 2014; 75(8):606–614. [PubMed: 24099506]

Scholl BJ, Leslie AM. Modularity, development and ‘theory of mind’. Mind & Language. 1999; 14:131–153.

Smith SM, Jenkinson M, Woolrich MW, Beckmann CF, Behrens TEJ, Johansen-Berg H, Bannister PR, De Luca M, Drobnjak I, Flitney DE, Niazy R, Saunders J, Vickers J, Zhang Y, De Stefano N,

Brady JM, Matthews PM. Advances in functional and structural MR image analysis and implementation as FSL. NeuroImage. 2004; 23(S1):208–219.

Sporns O, Honey CJ, Kötter R. Identification and classification of hubs in brain networks. PloS One. 2007; 2(10):e1049. [PubMed: 17940613]

Stern ER, Fitzgerald KD, Welsh RC, Abelson JL, Taylor SF. Resting-state functional connectivity between fronto-parietal and default mode networks in obsessive-compulsive disorder. PloS One. 2012; 7(5):e36356. [PubMed: 22570705]

Szeszko PR, Christian C, MacMaster F, Lencz T, Mirza Y, Taormina SP, Easter P, Rose M, Michalopoulou GA, Rosenberg DR. Gray matter structural alterations in psychotropic drug-naïve pediatric obsessive-compulsive disorder: An optimized voxel-based morphometry study. Am J Psychiatry. 2008; 165:1299–1307. [PubMed: 18413702]

Telesford QK, Simpson SL, Burdette JH, Hayasaka S, Laurienti PJ. The brain as a complex system: using network science as a tool for understanding the brain. Brain Connectivity. 2011; 1(4):295–308. [PubMed: 22432419]

Triggs WJ, McCoy KJM, Greer R, Rossi F, Bowers D, Kortenkamp S, Nadeau SE, Heilman KM, Goodman WK. Effects of left frontal transcranial magnetic stimulation on depressed mood, cognition, and corticomotor threshold. Biol Psychiatry. 1999; 45:1440–1446. [PubMed: 10356626]

van den Heuvel MP, Hulshoff Pol HE. Exploring the brain network: a review on resting-state fMRI functional connectivity. Eur Neuropsychopharmacol. 2010; 20(8):519–534. [PubMed: 20471808]

van den Heuvel OA, Veltman DJ, Groenewegen HJ, Witter MP, Cath DC, van Balkom AJ, van Hartskamp J, van Dyck R. Disorder-specific neuroanatomical correlates of attentional bias in obsessive-compulsive disorder, panic disorder, and hypochondriasis. Arch Gen Psychiatry. 2005; 62(8):922–933. [PubMed: 16061770]

Van Dijk KR, Hedden T, Venkataraman A, Evans KC, Lazar SW, Buckner RL. Intrinsic functional connectivity as a tool for human connectomics: theory, properties, and optimization. J Neurophysiol. 2010; 103:297–321. [PubMed: 19889849]

Venkatasubramanian G, Zutshi A, Jindal S, Srikanth SG, Kovoor JM, Kumar JK, Janardhan Reddy YC. Comprehensive evaluation of cortical structure abnormalities in drug-naive, adult patients with obsessive-compulsive disorder: a surface-based morphometry study. J Psychiatric Res. 2012; 46(9):1161–1168.

Viard A, Flament MF, Artiges E, Dehaene S, Naccache L, Cohen D, Mazet P, Mouren MC, Martinot JL. Cognitive control in childhood-onset obsessive–compulsive disorder: a functional MRI study. Psychol Med. 35:1007–1017.

Watts DJ, Strogatz SH. Collective dynamics of ‘small-world’ networks. Nature. 1998; 393(6684):440–442. [PubMed: 9623998]

Wechsler, D. Manual for the Wechsler Abbreviated Scale of Intelligence. Psychological Corporation; San Antonio: 1999.

Yamanishi T, Nakaaki S, Omori IM, Hashimoto N, Shinagawa Y, Hongo J, Horikoshi M, Tohyama J, Akechi T, Soma T, Iidaka T, Furukawa TA. Changes after behavior therapy among responsive and nonresponsive patients with obsessive-compulsive disorder. Psychiatry Res: Neuroimaging. 2009; 172:242–250. [PubMed: 19346109]

Yücel M, Harrison BJ, Wood SJ, Fornito A, Wellard RM, Pujol J, Clarke K, Phillips ML, Kyrios M, Velakoulis D, Pantelis C. Functional and biochemical alterations of the medial frontal cortex in obsessive-compulsive disorder. Arch Gen Psychiatry. 2007; 64(8):946–955. [PubMed: 17679639]

Zalesky A, Fornito A, Bullmore ET. Network-based statistic: Identifying differences in brain networks. NeuroImage. 2010; 53(4):1197–1207. [PubMed: 20600983]

Zhang T, Wang J, Yang Y, Wu Q, Li B, Chen L, Yue Q, Tang H, Yan C, Lui S, Huang Z, Chan RCK, Zang Y, He Y, Gong Q. Abnormal small-world architecture of top–down control networks in obsessive–compulsive disorder. J Psychiatry Neurosci. 2011; 36(1):23–31. [PubMed: 20964957]

Highlights

- The global brain resting-state fMRI graph-theory parameter small-worldness is lower in OCD than in healthy control children suggesting less efficient brain networking in pediatric OCD
- The global graph-theory parameter modularity is lower in OCD children suggesting alternative modular brain organization in pediatric OCD
- The local graph theory parameter clustering coefficient is higher in OCD children in sensorimotor cortex, supplementary motor cortex, and frontal pole suggesting realtive isolation of these brain regions
- The local graph theory parameter betweenness centrality is lower in OCD children in these same regions again suggesting relative isolation of these regions

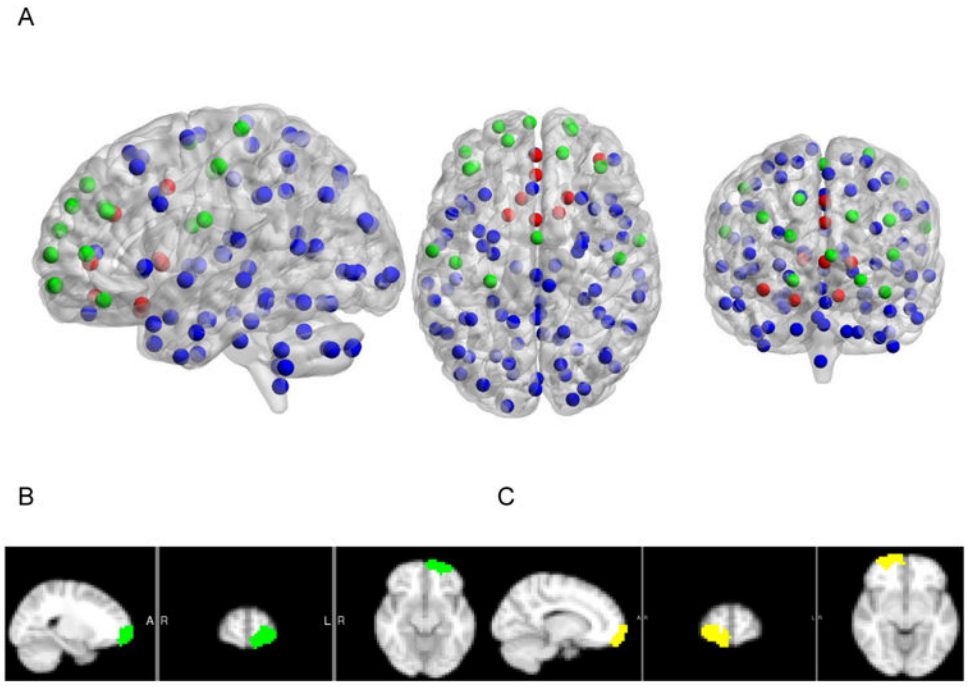

Fig. 1.

Nodes for global and local graph-theory analyses and frontopolar effects of OCD. Volume-rendered translucent brain in sagittal, axial, and coronal views displaying centers-of-gravity of 100 functional nodes for calculating global graph-theory measures. First-group nodes (see text) are green, second-group nodes red, third-group nodes blue (A). Nodes 80 (green; B) in left frontopolar cortex and 66 (yellow; C) in right frontopolar cortex had 20-35% higher group-mean clustering coefficent (indexing localized functional connectivity) in pediatric OCD patients than in healthy control children. A third node (56, not shown) in left frontopolar cortex had higher clustering coefficient and lower (-63.6%) betweenness centrality (indexing pass-through functional connectivity) in OCD than in controls. Other sites of elevated clustering coeffivcient included midline supplementary motor cortex and left sensorimotor cortex.

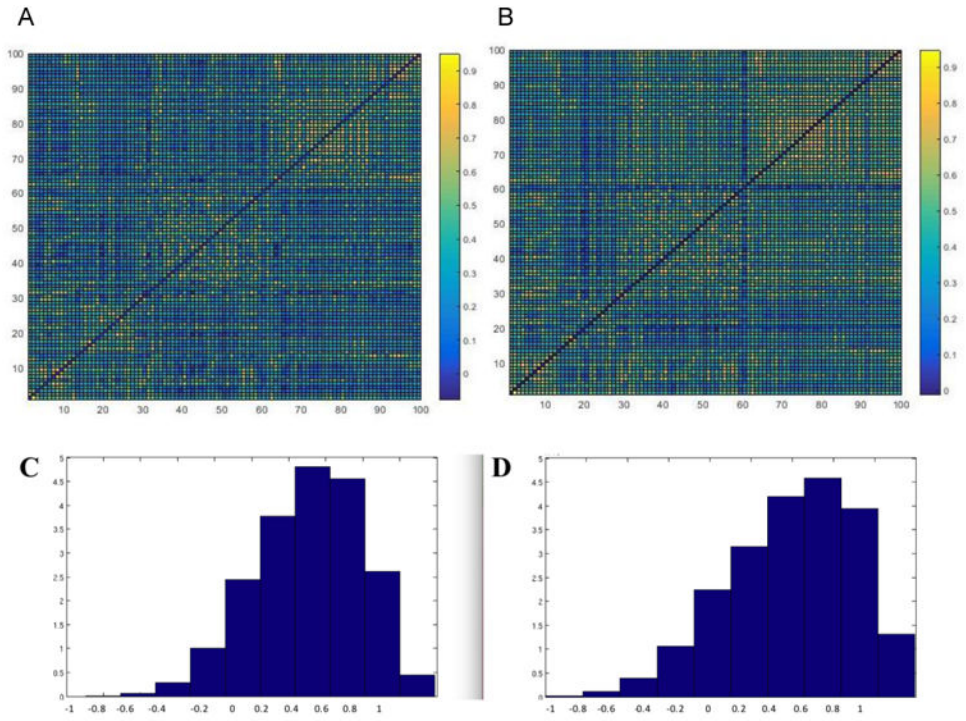

Fig. 2.

fMRI correlation matrices and histograms. Matrices representing Pearson r for correlations between all 100 anatomically arrayed functional nodes during 8-min whole-brain BOLD rsfMRI acquisition. Values averaged across healthy control (A) and OCD (B) groups. Color bars indicate magnitude of r. Histograms of r values for control (C) and OCD (D) groups. The two group distributions were normal and overlapping.

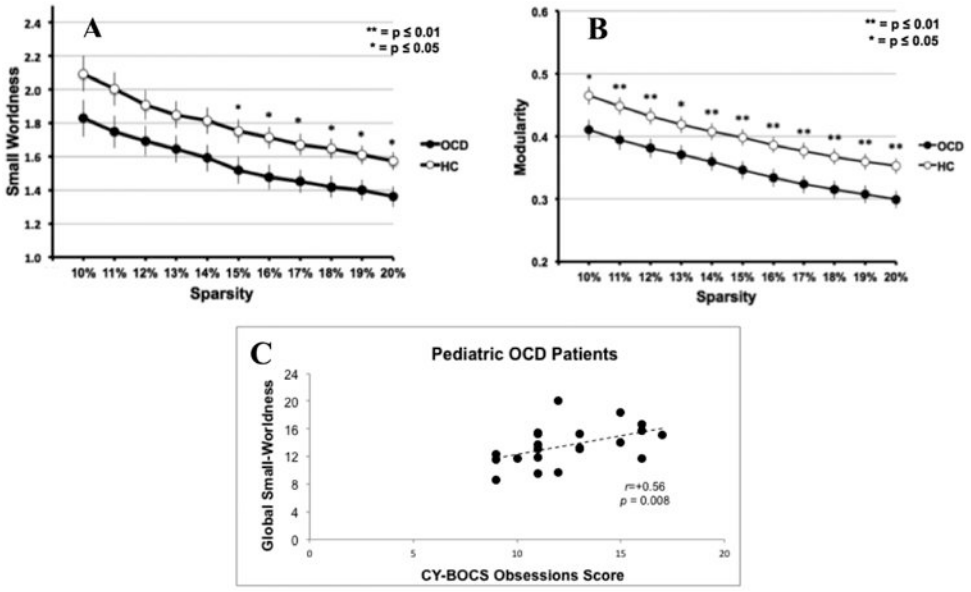

Fig. 3.

Effects of OCD and OCD symptoms on global graph-theory metrics. Group-mean values for the global rsfMRI network connectivity parameters small-worldness (A) and modularity (B) across the 10-20% of strongest connections (sparsity) for children with (filled circles) and without (open circles) OCD. Note significantly lower small-worldness (for sparsities >15%) and modularity (all sparsities) for the OCD group. Significant between-group differences at individual sparsity values are marked (*P<0.05, **P<0.01). For the overall areas-under-the-curve (AUCs), small-worldness was lower for the OCD group at P<0.05 and modularity was lower at P<0.01 (Table 2). Small-worldness findings are consistent with less efficient global information transfer in the brain during the resting state in OCD; modularity findings are consistent with the brain being divided into fewer or into a different set of functional modules during the resting state in OCD. Within the pediatric OCD group, the CY-BOCS Obsessions subscore correlated positively with small-worldness (Spearman r=0.56, P=0.008) (C).

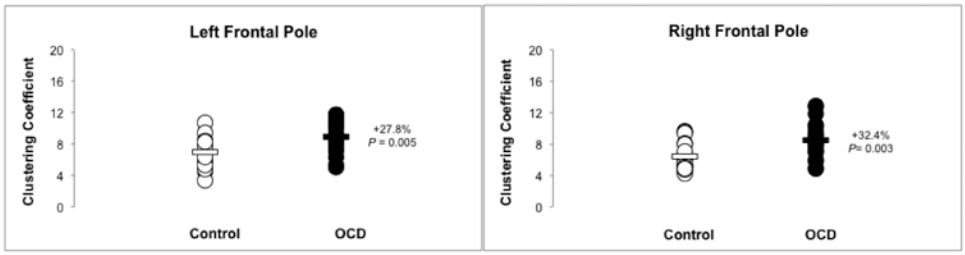

Fig. 4.

Effects of OCD and on local frontal polar graph-theory metrics. Single-subject (filled circles for patients, open circles for controls) and group-mean (bars) values for the local resting-state fMRI graph-theory metric clustering coefficient at left (Node 80) and right (Node 66) frontal poles for children with and without OCD. The OCD sample had significantly higher clustering coefficient at both sites. Higher clustering coefficient implies greater local connectivity of these nodes during the resting-state in OCD.

Table 1
Demographics and clinical characteristics of participants

Variables (mean±sd)	OCD	Healthy Controls	P
N (male/female)	21 ±13/8	20±11/9	0.654[a]
Age (years)	12.7±2.8	13.4±1.8	0.374[b]
CY-BOCS Obsessions	12.4±2.5		
CY-BOCS Compulsions	12.3±2.4		
CY-BOCS Total Score	24.7±2.4		

OCD, Obsessive-Compulsive disorder; CY-BOCS, Children's Yale-Brown Obsessive-Compulsive Scale

[a] P value obtained with χ^2 test

[b] P value obtained with independent T-test

Table 2
Global graph theory metrics of participants

Variables (mean±sd)/Nodes	OCD	Healthy Controls	p[a]
Global small-worldness	13.6±2.9	15.7±2.4	0.015
Global modularity	3.0±0.6	3.5±0.6	0.008
Global efficiency	6.6±0.6	6.6±0.8	0.890

OCD, Obsessive-Compulsive disorder

[a]P value obtained with protected post-hoc T-test following omnibus multivariate analysis-of-variance.

Significant findings in bold.

J Affect Disord. Author manuscript; available in PMC 2018 January 14.

Table 3

Local graph theory metrics for first-group nodes ("non-classical" OCD brain regions)

		MNI coordinates					
Brain Region	**Node**	**x**	**y**	**z**	**OCD**	**HC**	**P[a]**
					Local clustering coefficient		
Right frontal pole	66	19.4	62.8	-7.4	8.5±2.3	6.4±1.7	0.003
Left frontal pole	80	-20.5	61.6	-7.3	8.9±2.0	7.0±1.8	0.005
Right frontal pole	54	15.7	46.6	40.4	8.6±2.2	7.0±2.0	0.019
Left frontal pole	73	-15.5	53.6	30.4	8.1±1.8	7.0±1.8	0.073
Right frontal pole/middle frontal gyrus	47	37.4	38.5	29.8	8.3±1.9	7.1±1.4	0.033
Left frontal pole/middle frontal gyrus	2	-37.6	37.4	28.0	8.1±2.4	7.2±1.8	0.212
Right frontal pole	8	21.0	59.6	18.6	7.5±1.4	7.1±2.0	0.490
Left frontal pole	56	-34.9	38.9	-14.3	8.3±2.3	6.7±1.2	0.012
Left frontal pole	25	-39.7	47.0	7.6	7.6±1.7	7.2±1.4	0.472
Midline frontal pole	97	-3.1	63.8	7.2	7.1±2.0	7.2±2.5	0.929
Midline supplementary motor cortex	88	1.2	-1.7	61.0	8.4±1.9	6.7±1.5	0.003
Right post-central+precentral gyrus	71	48.0	-13.5	46.8	8.1±2.4	7.4±1.4	0.216
Left post-central+precentral gyrus	57	-45.2	-15.8	49.3	7.8±1.8	7.3±1.5	0.391
Right post-central+precentral gyrus	34[b]	59.2	-3.2	21.1	9.4±2.5	7.7±2.1	0.050
Left post-central+precentral gyrus	45	-58.4	-9.2	23.9	9.5±2.4	8.4±2.4	0.192
Left post-central+precentral gyrus	100	-25.5	-26.5	68.9	9.5±2.6	7.6±1.4	0.010
					Local betweenness centrality		
Right frontal pole	66[b]	19.4	62.8	-7.4	934±923	2067±1662	0.019
Left frontal pole	80[b]	-20.5	61.6	-7.3	477±862	1048±969	0.014
Right frontal pole	54	15.7	46.6	40.4	662±757	1201±923	0.059
Left frontal pole	73	-15.5	53.6	30.4	547±557	1113±1133	0.066
Right frontal pole/middle frontal gyrus	47	37.4	38.5	29.8	929±727	1257±1100	0.292
Left frontal pole/middle frontal gyrus	2	-37.6	37.4	28.0	853±845	959±1099	0.748
Right frontal pole	8	21.0	59.6	18.6	1103±1362	1544±1603	0.369
Left frontal pole	56	-34.9	38.9	-14.3	668±657	1834±1469	0.004
Left frontal pole	25	-39.7	47.0	7.6	1421±1489	1183±1013	0.560

Brain Region	Node	MNI coordinates x	y	z	OCD	HC	P[a]
Midline frontal pole	97	-3.1	63.8	7.2	1980±1972	1412±1274	0.291
Midline supplementary motor cortex	88[b]	1.2	-1.7	61.0	942±872	2004±1926	0.083
Right post-central+precentral gyrus	71	48.0	-13.5	46.8	1392±1515	1225±1544	0.735
Left post-central+precentral gyrus	57	-45.2	-15.8	49.3	1577±1595	1469±1437	0.829
Right post-central+precentral gyrus	34[b]	59.2	-3.2	21.1	470±525	1172±1142	0.024
Left post-central+precentral gyrus	45	-58.4	-9.2	23.9	441±525	525±710	0.280
Left post-central+precentral gyrus	100	-25.5	-26.5	68.9	288±418	710±718	0.039

OCD, Obsessive-compulsive disorder; HC, Healthy control.; MNI, Montréal Neurological Institute.

Endpoint values are subject group- AUC means ± standard deviation.

Note that node-generation does not always produce laterally symmetric brain node pairs.

[a]P value for T-test corrected for multiple comparisons with false discovery rate (FDR).

[b]Variable with non-normal distribution; data rank-transformed and tested non-parametrically.

Significant findings in bold.

Table 4

Local graph theory metrics for second-group nodes ("classical" OCD brain regions)

		MNI coordinates					
Brain Region	**Node**	**x**	**y**	**z**	**OCD**	**HC**	**P[a]**
					Local clustering coefficient		
Left orbitofrontal/subgenual cingulate	67	-7.5	20.5	-16.5	7.7±2.7	8.6±3.4	0.445
Right orbitofrontal cortex	78	18.6	21.0	-19.0	8.0±3.1	7.3±2.4	0.454
Right orbitofrontal cortex	20	36.9	42.8	-13.0	7.6±2.0	7.0±1.6	0.306
Right caudate	30	13.3	12.4	4.9	7.3±1.5	7.0±2.0	0.677
Left caudate/accumbens/putamen	98	-15.1	11.2	3.2	8.0±2.4	7.9±2.2	0.946
Midline posterior middle cingulate	69	0.4	8.6	39.4	7.8±1.4	7.0±1.9	0.163
Midline pregenual anterior cingulate	59	0.5	45.2	3.6	8.0±2.7	7.2±1.8	0.302
Midline anterior middle cingulate	95	0.4	34.0	26.8	7.1±1.8	6.0±1.9	0.098
					Local betweenness centrality		
Left orbitofrontal/subgenual cingulate	67	-7.5	20.5	-16.5	633±1021	655±883	0.950
Right orbitofrontal cortex	78	18.6	21.0	-19.0	1296±1492	561±468	0.075
Right orbitofrontal cortex	20	36.9	42.8	-13.0	1062±1493	1144±1154	0.850
Right caudate	30	13.3	12.4	4.9	1286±1571	1130±1125	0.734
Left caudate/accumbens/putamen	98	-15.1	11.2	3.2	862±996	370±353	0.062
Midline posterior middle cingulate	69	0.4	8.6	39.4	1597±1253	1350±1582	0.593
Midline pregenual anterior cingulate	59	0.5	45.2	3.6	1320±1243	703±740	0.069
Midline anterior middle cingulate	95	0.4	34.0	26.8	2209±2294	2257±3141	0.958

OCD, Obsessive-compulsive disorder; HC, Healthy control.; MNI, Montréal Neurological Institute.

Endpoint values are subject group- AUC means ± standard deviation.

Note that node-generation does not always produce laterally symmetric brain node pairs.

[a]P value obtained with T-test corrected for multiple comparisons with false discovery rate (FDR).

No significant effects of diagnosis in this node group.

In a third group of all remaining nodes in the brain (77), there were also no significant effects of diagnosis.